Polarization-maintaining optical fibers with low dispersion over a wide spectral range

Katsunari Okamoto, Malcolm P. Varnham, and David N. Payne

The total dispersion characteristics of the doubly clad Panda (or bow-tie) fibers have been investigated. It is shown that the contribution of the photoelastic effect to the total dispersion becomes of the order of several psec/km · nm in the 1.5–1.7-μm wavelength region. By careful adjustment of the cutoff wavelength, the total dispersion is reduced to within ±1 psec/km · nm over the 1.38–1.70-μm wavelength region for the HE_{11}^{x} mode and 1.38–1.68 μm for the HE_{11}^{y} mode, respectively.

I. Introduction

Single-mode fibers that can maintain a state of polarization are desirable for use in coherent optical fiber communication[1] and fiber-optic sensing systems.[2] On the other hand, double clad fibers, in which the waveguide dispersion is designed to cancel out the material dispersion over an extended spectral range, are of interest for use in wavelength division multiplexing systems and nonlinear optics.[3] Several independent theoretical and experimental investigations have been reported on birefringent fibers[4–6] and doubly clad fibers.[7–9] However, birefringent double clad fibers have to date not been investigated.

In this paper we describe propagation characteristics of the double clad Panda[5] or bow-tie[6] fibers which can transmit optical signals in a stable, linear polarizaiton state with minimum signal distortion over a wide spectral range.

II. Basic Equation

Figure 1 shows the waveguide configuration and refractive-index profile of the fiber. The core and inner cladding are circular and the refractive index in the stress-applying part is matched with that of the cladding. Doubly clad Panda (or bow-tie) fibers will be called Ω fibers, since the refractive-index profile of the fiber resembles the Greek letter Ω [Fig. 1(b)]. The propagation constants for the HE_{11}^{x} and HE_{11}^{y} modes in birefringent single-mode fibers can be expressed as [10]

$$\beta_1 = \beta^{(0)} - \Gamma_1, \tag{1a}$$

$$\beta_2 = \beta^{(0)} - \Gamma_2, \tag{1b}$$

where $\beta^{(0)}$ denotes the propagation constant of the HE_{11} mode in the unstressed fiber. The Γ_i ($i = 1,2$) in Eq. (1) are given by

$$\Gamma_i = \omega\epsilon_0 \int_0^{2\pi}\int_0^{\infty} \mathbf{E}_i^* \cdot \mathbf{X}\mathbf{E}_i r dr d\theta, \tag{2}$$

where **E** and **X** represent the electric field vector and the small deviation of the dielectric tensor caused by anisotropic thermal stress, respectively. The stress contributions, Γ_i, are obtained from Eq. (2) as

$$\Gamma_1 = k[(C_1 + C_2)\sigma_{xo}X(v) + 2C_2\sigma_{yo}Y(v)], \tag{3a}$$

$$\Gamma_2 = k[2C_2\sigma_{xo}X(v) + (C_1 + C_2)\sigma_{yo}(Y(v)], \tag{3b}$$

where C_1 and C_2 denote the photoelastic coefficients,[11] σ_{xo} and σ_{yo} are the principal stresses at the core center. In deriving Eqs. (3), we have assumed that Poisson's ratio ν and Young's modulus E are constant in the entire cross section of the fiber.[12] $X(v)$ and $Y(v)$ in Eqs. (3) are given by

$$X(v) = \frac{\int_0^{2\pi}\int_0^{\infty} \sigma_x(r,\theta)p(r,\theta;v) r dr d\theta}{\sigma_{xo}\int_0^{2\pi}\int_0^{\infty} p(r,\theta;v) r dr d\theta}, \tag{4a}$$

$$Y(v) = \frac{\int_0^{2\pi}\int_0^{\infty} \sigma_y(r,\theta)p(r,\theta;v) r dr d\theta}{\sigma_{yo}\int_0^{2\pi}\int_0^{\infty} p(r,\theta;v) r dr d\theta}, \tag{4b}$$

where $p(r,\theta;v)$ denotes the power distribution and $\sigma_x(r,\theta)$ and $\sigma_y(r,\theta)$ represent the principal stress distributions in the fiber, respectively. The normalized frequency V is defined as

$$V = ka\sqrt{n_1^2 - n_3^2}, \tag{5}$$

The authors are with University of Southampton, Electronics Department, Southampton, Hampshire S09 5NH, U.K.

Received 23 April 1983.
0003-6935/83/152370-04$01.00/0.

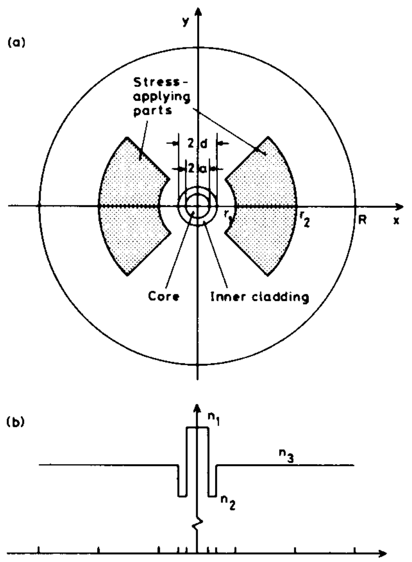

Fig. 1. Cross section (a) and refractive-index profile (b) of the Ω fiber. The refractive index of the stress-applying part is matched with the index of the cladding.

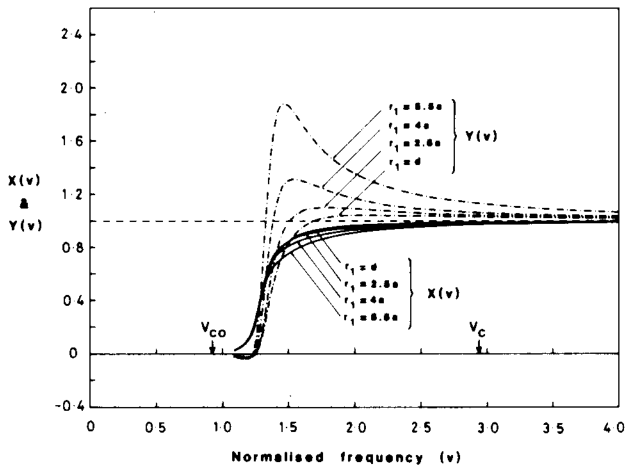

Fig. 2. $X(v)$ and $Y(v)$ in the Ω fiber with $\Delta_1 = 0.7\%$, $\Delta_2 = -0.5\%$, $2a = 5.3\ \mu m$ ($\lambda_c = 0.98\ \mu m$), $T = 0.4$, $R = 62.5\ \mu m$, and $r_2 = 0.5R$. The parameter r_1 is the inner radius of the stress-applying part.

where $k = 2\pi/\lambda$ and λ is the wavelength of light in vacuum. Using Eqs. (1), (3), and (4), the total dispersion in the fiber per unit length, per unit spectral width of the light source can be given by

$$\rho_1 = \frac{1}{\lambda C} k \frac{d^2\beta_1}{dk^2} = \frac{1}{\lambda C} k \frac{d^2\beta^{(0)}}{dk^2} - \frac{1}{\lambda C} k \frac{d^2\Gamma_1}{dk^2} = \rho^{(0)} - \gamma_1, \quad (6a)$$

$$\rho_2 = \frac{1}{\lambda C} k \frac{d^2\beta_2}{dk^2} = \frac{1}{\lambda C} k \frac{d^2\beta^{(0)}}{dk^2} - \frac{1}{\lambda C} k \frac{d^2\Gamma_2}{dk^2} = \rho^{(0)} - \gamma_2, \quad (6b)$$

where $\rho^{(0)}$ denotes the total dispersion in the unstressed fiber and γ_1 and γ_2 represent the stress contribution to the total dispersion for the HE_{11}^x and HE_{11}^y modes, respectively. The total dispersion $\rho^{(0)}$ in the unstressed fiber is given by the sum of the material and waveguide dispersion as[7]

$$\rho^{(0)} = \frac{1}{C}\left\{\lambda \frac{d^2n_1}{d\lambda^2}\frac{d(vb)}{dv} + \left[1 - \frac{d(vb)}{dv}\right]\lambda\frac{d^2n_3}{d\lambda^2}\right\} + \frac{N_1\Delta_1}{\lambda C} v \frac{d^2(vb)}{dV^2}, \quad (7)$$

where n_1 and n_3 denote the refractive indices of the core and cladding, and N_1 and Δ_1 represent the group index and the refractive-index difference of the core, respectively. The parameter $b(v)$ describes the dispersion characteristics of the mode, which is defined by

$$b(v) = \frac{[\beta^{(0)}/k]^2 - n_3^2}{n_1^2 - n_3^2}. \quad (8)$$

Although the refractive index n_2 of the inner cladding does not appear in Eqs. (7) and (8) explicitly, it affects the v-value dependence of $\beta^{(0)}$ and therefore contributes to $\rho^{(0)}$. The stress contributions γ_1 and γ_2 are obtained from Eqs. (3) and (6) as

$$\gamma_1 = \frac{1}{\lambda C}[(C_1 + C_2)\sigma_{x0}F_x(v) + 2C_2\sigma_{y0}F_y(v)], \quad (9a)$$

$$\gamma_2 = \frac{1}{\lambda C}[2C_2\sigma_{x0}F_x(v) + (C_1 + C_2)\sigma_{y0}F_y(v)], \quad (9b)$$

where

$$F_x(v) = v\frac{d^2(vX)}{dv^2}, \quad (10a)$$

$$F_y(v) = v\frac{d^2(vY)}{dv^2}. \quad (10b)$$

Since the dispersion of the photoelastic coefficients C_1 and C_2 in the 1.0–1.7-μm region are small compared with the other terms,[13] they have been neglected in the derivation of Eqs. (9).

In the numerical analysis of $X(v)$ and $Y(v)$, the principal stress distributions $\sigma_x(r,\theta)$ and $\sigma_y(r,\theta)$ are calculated by the finite-element method,[14] and $F_x(v)$ and $F_y(v)$ are obtained by numerical differentiation.

III. Dispersion Characteristics

In the following the contribution of the photoelastic effect is first examined and the total dispersion of the unstressed doubly clad fiber is briefly reviewed. The dispersion characteristic of the Ω fiber is then investigated taking the photoelastic effect into consideration.

Figure 2 shows the v-value dependence of $X(v)$ and $Y(v)$ for the Ω fiber calculated by using the following parameters: the index difference between core and cladding $\Delta_1 = (n_1^2 - n_3^2)/2n_1^2 = 0.7\%$ and that between the inner cladding and the outer $\Delta_2 = (n_2^2 - n_3^2)/2n_3^2 = -0.5\%$, the diameter of the core $2a = 5.3\ \mu m$, and the thickness ratio of the inner cladding to the outer $T = (d - a)/d = 0.4$. Cutoff v-value for the fundamental HE_{11} mode is $v_{co} = 0.924$ and that for the second-order mode is $v_c = 2.940$, respectively. In Fig. 2 and throughout this paper, r_1 is varied from $r_1 = a/(1 - T) = d$ to $r_1 = 5.5a$ and r_2 is kept constant as $r_2 = 0.5R$ where $R (= 62.5\ \mu m)$ is the radius of the fiber. The inner cladding and stress-applying part consist of fluoride glass and B_2O_3–GeO_2–SiO_2 glass, respectively. We have taken $C_1 = 7.42 \times 10^{-6}\ mm^2/kg$, $C_2 = 4.10 \times 10^{-5}\ mm^2/kg$, $E = 7830\ kg/mm^2$, and $\nu = 0.186$ in the calculation of the photoelastic effect.

Since the thermal expansion coefficient and the wavelength dispersion characteristics of the fluoride

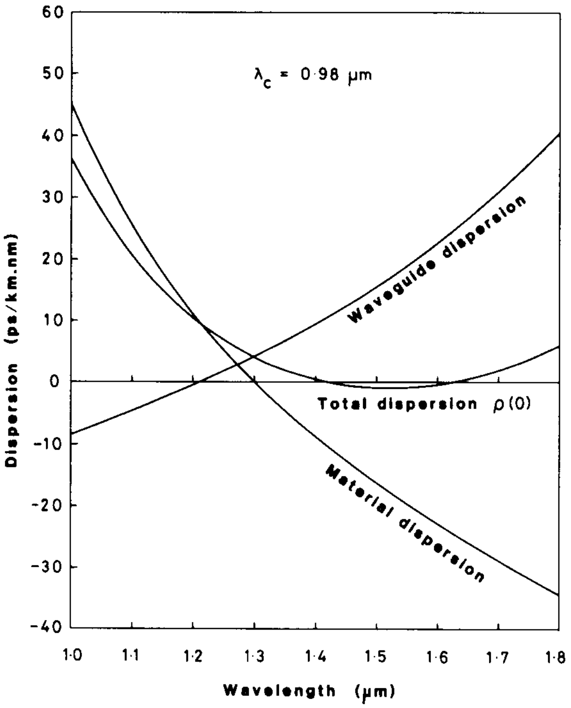

Fig. 3. Waveguide, material, and total dispersion for the Ω fiber when the photoelastic effect is ignored $[X(v) = Y(v) = 0]$. Parameters are the same as those used in Fig. 2.

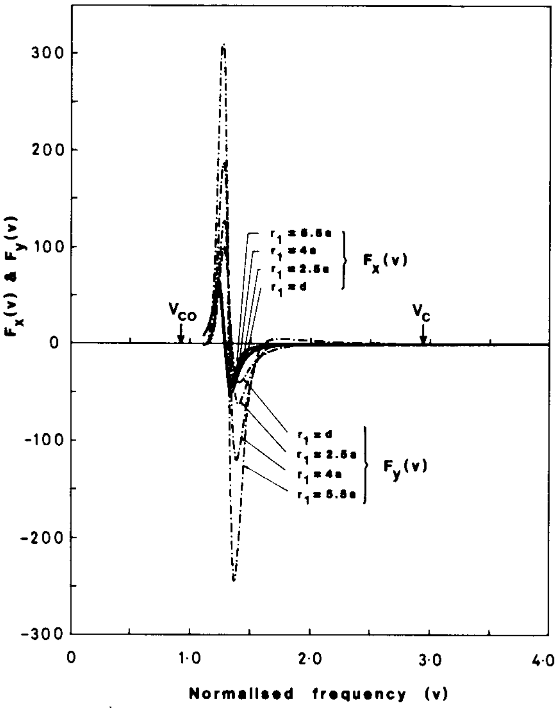

Fig. 4. $F_x(v)$ and $F_y(v)$ in the Ω fiber with the waveguide structure shown in Fig. 2.

glass are almost the same as those of silica glass, the data of silica glass have been used.[15,16]

Figure 2 shows that $X(v)$ and $Y(v)$ vary considerably in the small v-value region and that the dispersion of the photoelastic effect cannot be neglected. Figure 3 shows the total dispersion of the unstressed fiber $[X(v) = Y(v) = 0]$ having the above waveguide parameters together with material and waveguide dispersion.[7,8] The total dispersion is reduced to within ±1 psec/km · nm over the 1.38–1.66-μm wavelength range when the cutoff wavelength $\lambda_c = 0.98\ \mu$m. The stress contribution functions $F_x(v)$ and $F_y(v)$ are shown in Fig. 4. It is known from Fig. 4 that $F_x(v)$ and $F_y(v)$ are small and their influence to the total dispersion can be neglected in the large v-region. However, since the cutoff wavelength is determined as $\lambda_c = 0.98\ \mu$m, the v-value becomes small in the low-loss wavelength region of 1.5–1.7 μm. As shown in Fig. 4, $F_x(v)$ and $F_y(v)$ becomes fairly large in the small v-region. Therefore, the influence of stress to the total dispersion cannot be neglected in the Ω fibers.

Figures 5 and 6 show the total dispersion characteristics for the HE_{11}^x and HE_{11}^y modes of the Ω fibers having the same waveguide parameters used in Fig. 2 except for the core diameter (cutoff wavelength).

Figures 5 and 6 show that the stress contributions γ_1 and γ_2 are the order of several psec/km · nm in the 1.5–1.7-μm wavelength region. In Figs. 5 and 6, the core diameter is determined to be $2a = 5.4\ \mu$m ($\lambda_c = 1.0\ \mu$m) such that the total dispersion ρ_1 or ρ_2 is minimized within ±1 psec/km · nm for the inner radius of stress part $r_1 = 4a$. Although the waveguide dispersion of the unstressed fiber is very sensitive to the cutoff wavelength, the wavelength dependence of stress contributions γ_1 and γ_2 is almost the same for two cutoff wavelengths. For the present cutoff wavelength, the absolute value of total dispersion in the unstressed fiber $\rho^{(0)}$ is larger than 1 psec/km · nm between the 1.44- and 1.63-μm wavelength region. However, the total dispersion including the stress contribution is reduced to within ±1 psec/km · nm over the 1.38–1.70-μm wavelength range for the HE_{11}^x mode and over the 1.38–1.68-μm wavelength range for the HE_{11}^y mode, respectively, for $r_1 = 4a$.

Although the total dispersion characteristics in Figs. 5 and 6 are optimized for the waveguide structure with $r_1 = 4a$, it is possible to reduce the total dispersion below ±1 psec/km · nm for other waveguide structures with different r_1 by adjusting the cutoff wavelength properly. The group velocity for the optimized Ω fiber ($r_1 = 4a$) is almost constant over the 1.38–1.70-μm wavelength range; that is, the maximum difference of the group velocity is below 0.15 nsec/km in the above spectral region for both polarization modes. This gives a great deal of advantage for use in nonlinear fiber optics because the stable polarization state and the group velocity matching between the interacting waves make it possible to obtain long, effective interactions in the fiber.[3]

IV. Conclusion

In conclusion, we have reported the propagation characteristics of the Ω fibers (the doubly clad Panda or bow-tie fibers) taking the photoelastic effect into consideration. Since the cutoff wavelength of the Ω fibers is shorter than the conventional Panda or bow-tie fibers, the influence of stress to the total dispersion

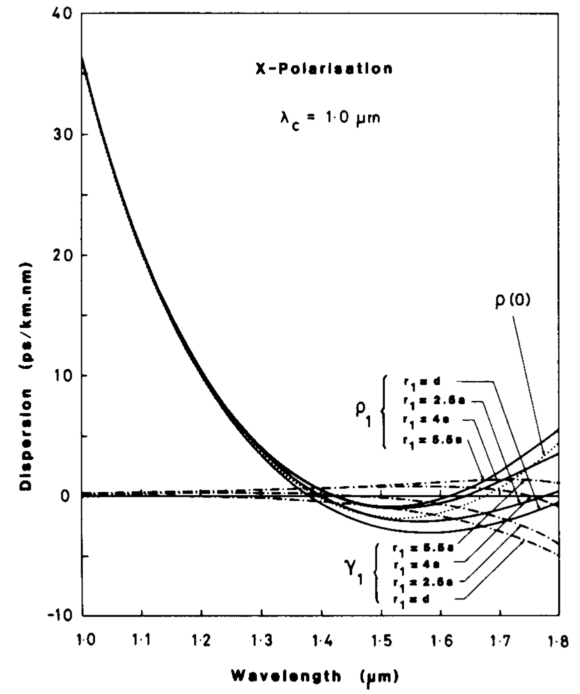

Fig. 5. Total dispersion characteristics for the HE^x_{11} mode in the Ω fiber. Core diameter is changed to $2a = 5.4$ μm ($\lambda_c = 1.0$ μm) such that the total dispersion is optimized for $r_1 = 4a$.

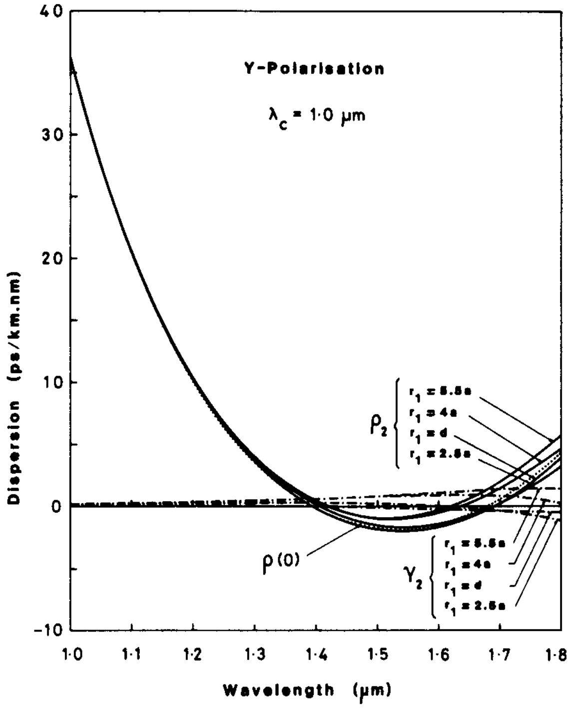

Fig. 6. Total dispersion characteristics for the HE^y_{11} mode in the Ω fiber having the same parameters as Fig. 5.

cannot be neglected in the low-loss 1.5–1.7-μm wavelength region. We have investigated the total dispersion characteristics of the typical Ω fiber with $\Delta_1 = 0.7\%$, $\Delta_2 = -0.5\%$, $2a = 5.4$ μm, and $T = 0.4$. It is shown that the stress contribution becomes of the order of several psec/km · nm in the 1.5–1.7-μm wavelength region. By determining the cutoff wavelength properly, the total dispersions are reduced to within ±1 psec/km · nm over the 1.38–1.70-μm wavelength region for the HE^x_{11} mode and over the 1.38–1.68-μm wavelength region for the HE^y_{11} mode, respectively.

The authors would like to thank T. Edahiro, NTT, Japan, for his suggestion of this work and A. H. Hartog and A. J. Barlow for helpful discussions. A Research Studentship (MPV) was provided by British Aerospace, and a Research Fellowship by the Pirelli General Cable Company (DNP). One of the authors (KO) is on leave from the NTT Ibaraki Electrical Communication Laboratory, Japan.

References

1. T. Okoshi, in *Technical Digest, Third Internatinal Conference on Integrated Optics and Optical Fiber Communication* (Optical Society of America, Washington, D.C., 1981), paper TUB1.
2. R. Ulrich and M. Johnson, Opt. Lett. **4,** 152 (1979).
3. Y. Ohmori and Y. Sasaki, IEEE J. Quantum Electron **QE-18,** 758 (1982).
4. V. Ramaswamy, I. P. Kaminow, and P. Kaiser, Appl. Phys. Lett. **33,** 814 (1978).
5. T. Hosaka, K. Okamoto, T. Miya, Y. Sasaki, and T. Edahiro, Electron. Lett. **17,** 530 (1981).
6. R. D. Birch, D. N. Payne, and M. P. Varnham, Electron. Lett. **18,** 1036 (1982).
7. K. Okamoto, T. Edahiro, A. Kawana, and T. Miya, Electron. Lett. **15,** 729 (1979).
8. T. Miya, K. Okamoto, Y. Ohmori, and Y. Sasaki, IEEE J. Quantum Electron **QE-17,** 858 (1981).
9. S. J. Jang, L. G. Cohen, W. L. Mammel, and M. S. Saifi, Bell Syst. Tech. J. **61,** 385 (1982).
10. K. Okamoto, T. Edahiro, and N. Shibata, Opt. Lett. **7,** 569 (1982).
11. W. Primak and D. Post, J. Appl. Phys. **30,** 779 (1959).
12. G. W. Scherer, Appl. Opt. **19,** 2000 (1980).
13. N. K. Sinha, Phys. Chem. Glasses **19,** 69 (1978).
14. K. Okamoto, T. Hosaka, and T. Edahiro, IEEE J. Quantum Electron. **QE-17,** 2123 (1981).
15. A. Muhlich, K. Rau, F. Simmat, and N. Treber, "A New Doped Synthetic Fused Silica as Bulk Material for Low-Loss Optical Fibers," in *Technical Digest, First European Conference on Optical Communication*, London (1975).
16. A. H. Hartog, U. Southampton; unpublished work.